Proceedings of the 7th International Conference on Gas Hydrates (ICGH 2011)
Edinburgh, Scotland, United Kingdom, July 17-21, 2011.

ACOUSTIC DETERMINATION OF METHANE HYDRATE DISSOCIATION PRESSURES

Chad A. Greene* and Preston S. Wilson
Applied Research Laboratories
The University of Texas at Austin
Austin, TX
UNITED STATES

Richard B. Coffin
Naval Research Laboratory
Washington, DC
UNITED STATES

ABSTRACT

The unique nature of the molecular structures of gas hydrates results in curious acoustic properties which have yet to be adequately characterized. Understanding the acoustic behavior of hydrates in liquids, in bubbly liquids, and in sediments containing liquids and/or gas is vital for surveying their location using seismic or echosounding techniques and may become a key tool for monitoring hydrate dissociation and its possible link to climate change. Acoustic properties of gassy substances are known to have a strong dependence on excitation frequency; however, tabulated values of hydrate sound speeds are most often measured at high frequencies (>200 kHz) despite modern location methods which use frequencies below 100 kHz. This presentation details a laboratory experiment in which the dissociation pressures of natural structure I and structure II methane hydrate samples were determined by measuring their low-frequency acoustic velocity in a liquid as a function of hydrostatic pressure. [Work supported by The United States Office of Naval Research.]

Keywords: low-frequency acoustics, phase mapping, hydrate stability, sound propagation

NOMENCLATURE

c	speed of sound
f	frequency
G	shear modulus
K	bulk modulus
L	resonator length
n	mode number
P	hydrostatic pressure
S	salinity
sI	structure I gas hydrate
sII	structure II gas hydrate
T	temperature
VSA	vector signal analyzer
λ	acoustic wavelength
ρ	density
χ	volume fraction

INTRODUCTION

Gas hydrates are often formed and found in ocean sediments along continental margins. The compounds are also known to form as a skin on rising methane bubbles, as reported by Rehder et al. [1], Heeschen et al. [2], and Sauter et al. [3]. To improve seismic detection and characterization of hydrates, it is necessary to gain a better understanding of their acoustic behavior in the variety of media in which they are found. Of particular import is low-frequency acoustic behavior of hydrates, which has yet to see extensive investigation. As a step toward a better understanding of the behavior of hydrates in acoustically complex media such as in water-saturated sed-

Report Documentation Page

Form Approved
OMB No. 0704-0188

1. REPORT DATE	2. REPORT TYPE	3. DATES COVERED
JUL 2011		**00-00-2011 to 00-00-2011**

4. TITLE AND SUBTITLE	5a. CONTRACT NUMBER
Acoustic Determination Of Methane Hydrate Disssociation Pressures	5b. GRANT NUMBER
	5c. PROGRAM ELEMENT NUMBER
6. AUTHOR(S)	5d. PROJECT NUMBER
	5e. TASK NUMBER
	5f. WORK UNIT NUMBER
7. PERFORMING ORGANIZATION NAME(S) AND ADDRESS(ES) **The University of Texas at Austin,Applied Research Laboratories,Austin,TX,78712**	8. PERFORMING ORGANIZATION REPORT NUMBER
9. SPONSORING/MONITORING AGENCY NAME(S) AND ADDRESS(ES)	10. SPONSOR/MONITOR'S ACRONYM(S)
	11. SPONSOR/MONITOR'S REPORT NUMBER(S)

12. DISTRIBUTION/AVAILABILITY STATEMENT
Approved for public release; distribution unlimited

13. SUPPLEMENTARY NOTES
Proceedings of the 7th International Conference on Gas Hydrates (ICGH 2011) Edinburgh, Scotland, United Kingdom, July 17-21, 2011,Government or Federal Purpose Rights License

14. ABSTRACT
The unique nature of the molecular structures of gas hydrates results in curious acoustic properties which have yet to be adequately characterized. Understanding the acoustic behavior of hydrates in liquids, in bubbly liquids, and in sediments containing liquids and/or gas is vital for surveying their location using seismic or echosounding techniques and may become a key tool for monitoring hydrate dissociation and its possible link to climate change. Acoustic properties of gassy substances are known to have a strong dependence on excitation frequency; however, tabulated values of hydrate sound speeds are most often measured at high frequencies (>200 kHz) despite modern location methods which use frequencies below 100 kHz. This presentation details a laboratory experiment in which the dissociation pressures of natural structure I and structure II methane hydrate samples were determined by measuring their low-frequency acoustic velocity in a liquid as a function of hydrostatic pressure.

15. SUBJECT TERMS

16. SECURITY CLASSIFICATION OF:			17. LIMITATION OF ABSTRACT	18. NUMBER OF PAGES	19a. NAME OF RESPONSIBLE PERSON
a. REPORT	b. ABSTRACT	c. THIS PAGE			
unclassified	**unclassified**	**unclassified**	**Same as Report (SAR)**	**11**	

iments, this work focuses on the low-frequency acoustic behavior of structure I and structure II methane hydrates in liquids and in bubbly liquids.

Definitions

Gas hydrates, often referred to as *clathrate hydrates*, *gas clathrates*, or simply, *hydrates*, are crystalline molecular host structures which entrap guest molecules without chemical bonds. The substance forms in high-pressure, low-temperature environments, and requires such conditions to remain stable. The multiple names for the compound are often used interchangeably; however, each term describes specific traits of the structure. Powell defined *clathrate*, from the Latin, *clathratus*, meaning, "to encage," as a general term for any such cage-like molecular structure [4]. A *clathrate hydrate* is then a compound in which water forms the rigid lattice, and *gas clathrate hydrate* specifies that the guest molecule in the structure is a gas. In this paper, the term *clathrate* will be dropped and the compounds will be referred to as *hydrates*, *gas hydrates*, or *methane hydrates*, dependent upon the appropriate level of generality or specificity. Three molecular structures of gas hydrates are known to exist. Structure I is a body-centered-cubic orientation which forms naturally in deep oceans from biogenic gases. It is worth noting that this molecular geometry can trap great quantities of gas in a small volume, concentrating methane by a factor of 164 relative to its volume at STP [5]. Structure II is a diamond lattice within a cubic framework, formed from thermogenic gases, often in oil-rich areas [6]. Structure H is a rare hexagonal form, which has only recently been shown to exist in nature [7]. The focus of the present work is on structure I and structure II hydrates hosting molecules of methane gas.

DESCRIPTION OF EXPERIMENT

A pressure- and temperature-controlled chamber was designed to investigate the effect of hydrostatic pressure on the acoustic properties of brines containing samples of methane hydrates. An annular cylindrical borosilicate resonator with inner diameter of 52 mm, outer diameter of 70 mm, and length 459 mm, was

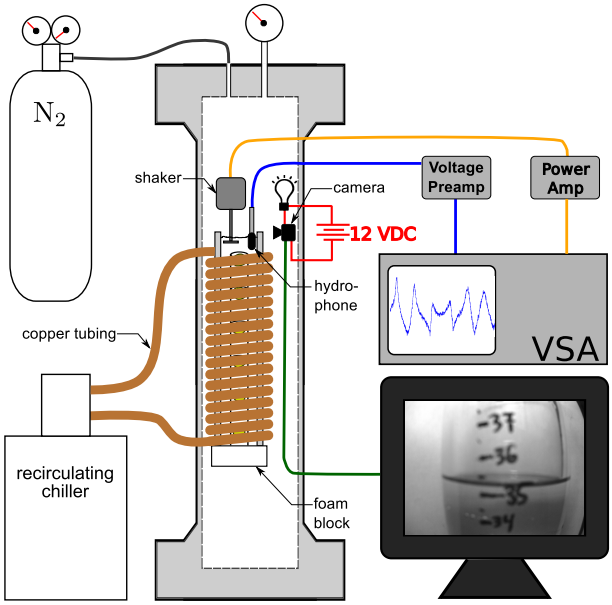

Figure 1: Schematic of the experimental apparatus.

wrapped in coiled copper tubing through which chilled ethylene glycol at a temperature of −20°C circulated. The exposed copper tubing was then covered with fiberglass insulation. The bottom of the resonator was sealed with a nitrile rubber membrane and the resonator rested atop an open-cell foam block, creating an approximately pressure-release boundary condition at the lower terminus. An audio amplifier powered an electromagnetic shaker, to which an aluminum piston was attached. The piston was placed near the top of the column of brine and oriented to excite longitudinal acoustic modes within the fluid enclosed by the resonator walls while a small laboratory hydrophone, with its cable encased in a water-filled stainless steel sheath, sensed the acoustic response of the system. The hydrophone signal was amplified and bandpass filtered with a voltage preamp. A vector signal analyzer (VSA) generated the acoustic signals (band-limited periodic chirps) and digitized the acoustic spectrum of the sample for each measurement. The apparatus and procedures used in the present work closely mimics the experimental design described by Wilson et al. in Ref. [8]. A schematic of the apparatus is given in Fig. 1.

A copper wire busbar cage, shown in Fig. 2, was constructed to suspend six approximately

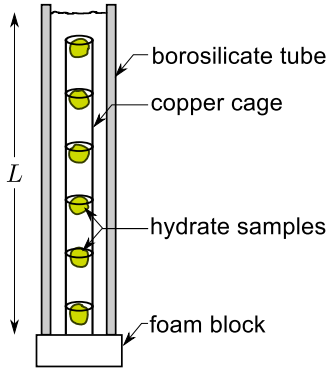

Figure 2: Schematic of borosilicate resonator with copper wire cage holding six hydrate samples. Open-cell foam is seen at the lower terminus of the resonator.

equally-spaced pieces of gas hydrate in the resonator. The samples float, so to keep them in place, the cage was wrapped in copper wire mesh. To prevent bubbles from attaching to the copper cage, the cage was coated with a hydroxy-terminated polydimethylsiloxane solution and allowed to dry before it was placed in the resonator.

Natural samples of methane hydrates were collected through coring operations between 1998 and 2000 and stored in liquid nitrogen at atmospheric pressure until January 2010. At that time, the hydrates were packed in a dewar with liquid nitrogen and shipped from the storage facility at the Naval Research Laboratory in Washington D.C. to Applied Research Laboratories in Austin, Texas. Geographical origins and molecular structures of the samples are listed in Table 1.

For each test, a hydrate sample was divided into six pieces, each approximately 2 cm in diameter, and placed in the copper cage. The cage was lowered into the pre-chilled resonator which was filled with a brine of salinity $S = 131 \pm 2‰$. With the resonator in place inside the pressure vessel, the piston of the shaker and hydrophone were positioned near the top of the brine, and the vessel was quickly sealed and pressurized with nitrogen to approximately 2.5 MPa. The height of the liquid column inside the resonator, L, was determined by viewing a video image from a camera placed inside the pressure vessel and aimed at the top of the resonator. The VSA recorded an acoustic spectrum given by the linear frequency-domain average of 30 transfer functions (between the hydrophone and excitation signals) over a frequency range which was determined based upon the resonance frequencies observed for each sample and hydrostatic pressure. After recording each spectrum, a small amount of gas was vented from the chamber to slightly reduce hydrostatic pressure in the vessel. Measurements were repeated at decrementing pressures until the acoustic signal was no longer discernible. Shifts in resonance frequencies were often observed during pressure reduction; however, no spectral changes were seen more than 10 seconds after pressure reduction. To ensure stability of the system, measurements were performed 120 seconds after each pressure reduction.

For each recorded spectrum, sound speed of the mixture was calculated by the slope method described in the following section, taking only the two lowest-frequency resonance peaks. At high hydrostatic pressures, several resonance peaks were distinct over the frequency range and a linear fit of the resonance frequencies versus mode number showed a low coefficient of determination. However, at low hydrostatic pressures, higher-mode resonances faded and became indistinguishable. Thus, for consistency, only the two lowest resonance frequencies were used for all spectra.

The experimental design was tested by measuring the sound speed of a brine ($S = 98‰$) chilled to -0.3℃. Without the copper wire sample holder in the resonator, in-resonator sound speed was measured as 1347 m/s. After accounting for the elastic waveguide effect of the borosilicate tube (described below), the freefield acoustic velocity of the brine was determined to be 1546 m/s, approximately 0.4% greater than the predicted value. This error is likely caused by uncertainties in the measurement of L or temperature in the column. Next, the empty copper cage was placed in the resonator with the brine and the measurement was repeated. The presence of the cage in the resonator had minimal effects on the overall structure of the acoustic spectrum of the water column, but resulted in

sample	structure	origin	T [°C]	CH_4 [%]	C_2H_6 [%]	C_3H_8 [%]	C_4H_{10} [%]
CMsI	I	Cascadia Margin	-8.3	99.79	0.21	-	-
CMsII	II	Cascadia Margin	-4.7	81.89	10.4	3.7	1.40
HMsI	I	Håkon Mosby	-6.2	99.49	0.14	0.12	0.15
GMsII	II	Gulf of Mexico	-6.5	29.67	15.35	36.61	13.61

Table 1: Structures, geographical origins, temperatures and compositions of hydrate samples. Compositions were determined using a Varian Saturn 2200 mass spectrometer, then quantitatively determined with a Varian CP 3800 gas chromatograph, as described in Ref. [9]. Percentages of butane and isobutane have been combined in the C_4H_{10} column.

a 0.3% decrease in the measured sound speed of the brine.

EXPERIMENTAL MODELS AND DATA ANALYSIS

Measurements performed in the present experiment employed an apparatus known in the acoustics community as a one-dimensional acoustic resonator or waveguide. Sound speeds of hydrate/brine mixtures measured in the resonator were numerically corrected to account for a well-known systematic error due do elasticity of the resonator walls, then the data was further analyzed to extract material properties of the hydrate samples using Wood's model of sound propagation through multiphase mixtures. Changes in sound speeds of the mixtures observed as a function of changes in hydrostatic pressure offer clear measurements of phase boundaries, and are in rough agreement with established hydrate stability models.

1-D Resonator Sound Speed Measurement

The low-frequency sound speed of a fluid can be measured by determining the resonance frequencies of the fluid sample inside an acoustic waveguide. This technique facilitates laboratory measurements at low frequencies because the resonator length need only be one-half acoustic wavelength, as compared to time-of-flight measurements, which require sample lengths equivalent to several wavelengths. In the present model, the inner walls of the borosilicate tube are assumed to be rigid and the ends are approximated as pressure-release boundary conditions. Temporarily neglecting the elasticity of the borosilicate tube, the expression for the eigenfrequencies of the resonator, $f_n = \frac{nc}{2L}$, where n is the mode number and L is the length of the resonator, yields an expression for the sound speed of the fluid mixture,

$$c = 2L\frac{\Delta f_n}{\Delta n}, \tag{1}$$

where $\Delta f_n/\Delta n$ is the slope of the line given by a linear least squares fit of the measured resonance frequencies versus mode number. Returning now to the finite elasticity of the wall material, the effect of the wall elasticity is seen as a reduction in sound speed relative to that which would be observed in an unconfined volume of the same material, often called the "free field." An exact analytical model of sound propagation through a finite-thickness elastic-walled, fluid-filled cylindrical tube is described in Ref. [10]. The present work involves two types of measurements. The first is acoustic measurement of hydrate dissociation pressures, which relies on relative changes in sound speed due to the presence of gas bubbles. For determination of dissociation pressures, the apparent sound speeds observed inside the resonator were adequate, and the correction for the elastic waveguide effect was not applied. Hydrate bulk moduli were also measured using the low-frequency acoustic technique. For these material property measurements, it was necessary to correct for the elasticity of the tube walls using the procedure described in Ref. [11].

Wood's Model of Sound Propagation Through Multiphase Mixtures

Measurement capabilities of an acoustic resonator extend beyond the simple determination of the speed of sound in a single fluid medium—Material properties of individual constituents

in a multiphase mixture may also be obtained through the use of Wood's model, which is described here. A fluid medium may be approximated as an acoustically-homogeneous mixture if all particles constituting the mixture are much smaller in dimension than an acoustic wave traveling through the mixture, the particles are evenly distributed throughout the mixture, and the particles number $\gg 1$ per wavelength. By this definition, a two-phase medium consisting of a liquid hosting a distribution of gas bubbles or solid particles may be approximated as a bulk medium with an effective bulk modulus K_m and density ρ_m. The effective properties of the mixture are obtained as a linear combination its constituent properties by their volumes,

$$K_\mathrm{m} = \frac{K_1 K_2}{\chi K_1 + (1-\chi) K_2} \tag{2}$$

and

$$\rho_\mathrm{m} = (1-\chi)\rho_1 + \chi\rho_2, \tag{3}$$

where K_1 and K_2 are the bulk moduli of the liquid and guest particles, respectively, and ρ_1 and ρ_2 are the densities of the liquid and guest particles. The volume fraction χ of the guest is given by

$$\chi = \frac{V_2}{V_1 + V_2}, \tag{4}$$

where V_2 and V_1 are the total respective volumes of the guest particles and host liquid in the resonator. Wood's model [12] of sound speed through the mixture is then found as a function of the bulk modulus and density of the effective medium,

$$c_\mathrm{m} = \sqrt{\frac{K_\mathrm{m}}{\rho_\mathrm{m}}}, \text{ or,} \tag{5}$$

$$c_\mathrm{m} = \sqrt{\frac{K_1 K_2 [(1-\chi)\rho_1 + \chi\rho_2]^{-1}}{\chi K_1 + (1-\chi) K_2}}. \tag{6}$$

Similarly, Wood's model may also be employed to predict the sound speed of three-phase media such as the mixtures of seawater, gas, and solid hydrates which have been observed in nature. For the three-phase case, volume fractions χ_1, χ_2, and χ_3 are used describe the relative volumes of the guest particles in the mixture,

$$\chi_1 = \frac{V_1}{V_1 + V_2 + V_3} \tag{7}$$

$$\chi_2 = \frac{V_2}{V_1 + V_2 + V_3} \tag{8}$$

$$\chi_3 = \frac{V_3}{V_1 + V_2 + V_3}. \tag{9}$$

The bulk modulus of the mixture is then

$$K_\mathrm{m} = \frac{K_1 K_2 K_3}{\chi_1 K_2 K_3 + \chi_2 K_1 K_3 + \chi_3 K_1 K_2}, \tag{10}$$

where K_1, K_2, and K_3 are the bulk moduli of the liquid host and the gas and solid guests, respectively. Likewise, the density of the three-phase mixture is

$$\rho_\mathrm{m} = \chi_1\rho_1 + \chi_2\rho_2 + \chi_3\rho_3. \tag{11}$$

The expressions for volume fractions, mixture bulk modulus, and mixture density then lead to an expression for the mean velocity of an acoustic wave traveling through the three-phase medium,

$$c_\mathrm{m} = \sqrt{\frac{K_1 K_2 K_3 [\chi_1\rho_1 + \chi_2\rho_2 + \chi_3\rho_3]^{-1}}{\chi_1 K_2 K_3 + \chi_2 K_1 K_3 + \chi_3 K_1 K_2}}. \tag{12}$$

Given this model and knowledge of the material properties of any two of the three constituents of the mixture, it is possible to then determine an unknown material property of the third constituent. For example, the bulk modulus and density of a water or brine host is well-established. Assuming a dissociating methane hydrate releases bubbles of methane gas into the mixture, tabulated properties of methane gas should suffice as values for K_2 and ρ_2. A simple laboratory measurement of the hydrate sample density then leaves one unknown value, K_3, which may be determined by rearranging Eq. 12 using measured values of C_m.

Hydrate Stability Models

In recent years, several groups have attempted to model the stability regimes of gas hydrates. Parrish and Prausnitz (Ref. [13]) used experimental data to fit constants to a model based on the work of Van der Waals and Platteeuw [14]. Parrish and Prausnitz stated that their model

model	relation
Parrish and Prausnitz, 1972	$\ln(P/101.325) = -1212.2 + 44344.0/T + 187.719 \ln T$
Dickens and Quinby-Hunt, 1994	$\frac{1}{T} = 3.79 \times 10^{-3} - 2.83 \times 10^{-4}[\log_{10}(P/1000)]$
Sloan, 1998	$P = \exp(38.98 - 8533.8/T)$
Peltzer and Brewer, 2000	$\frac{1}{T} = 3.83 \times 10^{-3} - 4.09 \times 10^{-4}[\log_{10}(P/1000)]...$ $+8.64 \times 10^{-5}[\log_{10}(P/1000)]^2$

Table 2: Hydrate stability models taken from the literature. Pressures are given in kilopascals and temperature is in units kelvin.

should only apply to structure I methane hydrates, and the model was validated for a temperature range of 0℃ to 27℃. Two decades later, Dickens and Quinby-Hunt developed an empirical equation based on data from their own experiments on methane hydrates in seawater of salinity $S = 33.5‰$ [15]. Sloan later gave a detailed explanation of the thermodynamic and kinetic properties of each of the three known structures of methane hydrates. In that paper he gives an expression for the temperature-dependent dissociation pressure of methane hydrate, but neglects to discuss how the relation was developed or which hydrate structure it describes [6]. Soon after, Peltzer and Brewer fit the data presented in Sloan's paper to a simple second-order polynomial to build an expression which was modeled after Dickens and Quinby-Hunt's relation [16]. The models are provided for reference in Table 2.

The four models discussed in this paper take various forms, but each describes an inverse relationship between the pressure and temperature of hydrate dissociation. Of these models, only the Parrish and Prausnitz model is structure-specific. Although some of the authors who developed the models listed in Table 2 acknowledged that the dissociation temperature-pressure relation will be affected when the hydrate is surrounded by seawater, only Dickens and Quinby-Hunt explicitly stated the salinity of the host liquid considered in the development of their models.

RESULTS

During the experiments on gas hydrate samples it was observed that the acoustic spectra captured at hydrostatic pressures above 500 kPa to 1000 kPa showed impressive signal-to-noise ratios with distinct peaks at resonance frequencies and deep valleys at antiresonances. Regularity of the intervals between resonances indicated a frequency-independent sound speed below 9 kHz, and a >50 dB difference between peak and valley receiver voltages implied a low-noise system with little acoustic loss. As hydrostatic pressure in the chamber decreased, the hydrates began to dissociate, gas formed on the samples, and the bubbles were released into the brine. The introduction of bubbles then lowered the effective sound speed of the bulk medium in the resonator, thus, shifting resonances lower in frequency. The rising bubbles in the column reduced signal-to-noise ratios, due in part to flow-generated noise, and due in part to the attenuation of acoustic energy by conversion into heat during oscillation of the excited bubbles. Measurements were discontinued when the acoustic signal was no longer discernible. The full data set and a detailed description of the experiment are presented in Ref. [17].

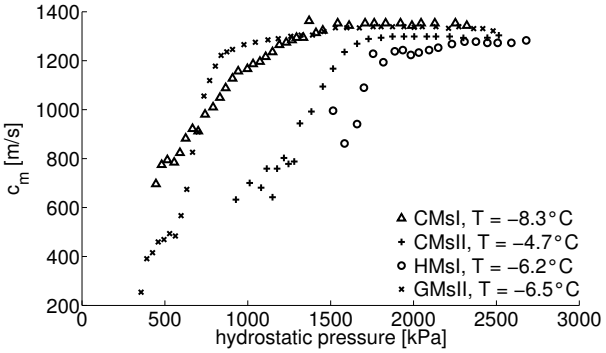

Figure 3: Measured low-frequency sound speeds of hydrate mixtures.

Measured values of in-resonator acoustic velocities for four brine mixtures containing the gas

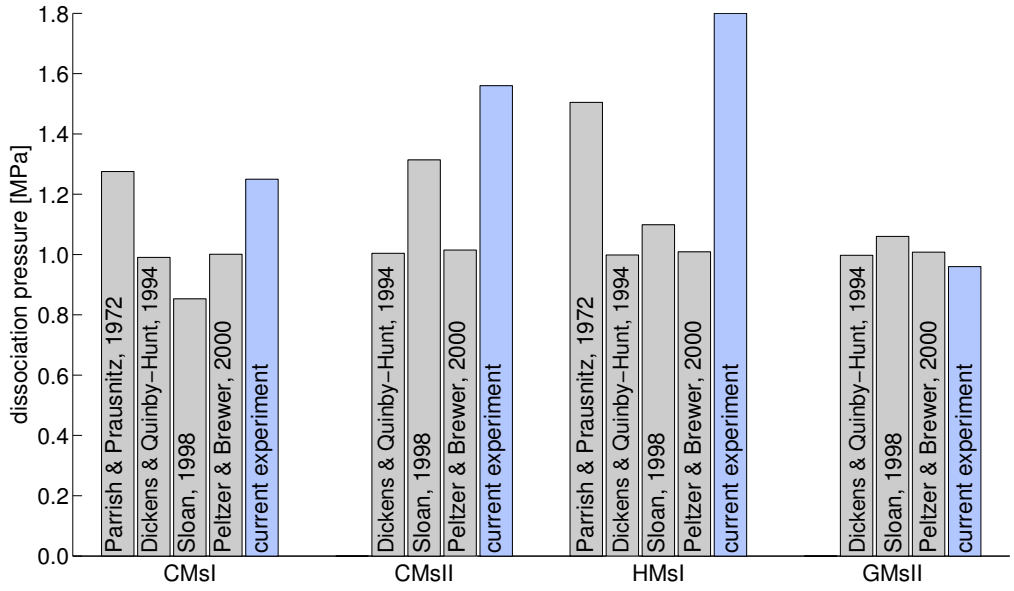

Figure 4: Acoustically-measured gas hydrate dissociation pressures compared to established models. The Parrish and Prausnitz model is only valid for comparison to results obtained for structure I hydrates. Most predicted values trend lower than dissociation pressures measured acoustically, possibly due to the models' neglect of salinity.

hydrate samples listed in Table 2 are presented in Fig. 3. These values were used only to determine the pressure at which the hydrate samples exited their stability regime, and thus, correction for the elastic waveguide effect of the borosilicate tube is unnecessary. Dissociation pressures were determined by interpolating the pressure at which c_{m} fell below 95% of the mean of the values of c_{m} corresponding to the ten highest-pressure data points for each sample. Dissociation was confirmed by a presence of bubbles observed via the video system at these pressures. Acoustically-determined dissociation pressures are presented in Fig. 4 alongside predictions determined by several common hydrate stability models. The Parrish and Prausnitz model applies only to structure I methane hydrates, and thus does not appear for comparison to experimental data of samples CMsII and GMsII.

Data presented in Fig. 3 were analyzed for relative changes in mixture sound speeds, thus, correction for the elasticity of the borosilicate tube was unnecessary for dissociation pressure measurements. Bulk moduli measurements were determined using values of c_{m} obtained for stable hydrate samples (where no bubbles were present in the tube), correcting c_{m} to account for the elastic waveguide effect, then calculating the sample bulk moduli using Eq. 6.

DISCUSSION

In Fig. 4 it is shown that for structure I hydrate samples, the Parrish and Prausnitz predictions appear to be outliers among the model predictions, possibly due to the sample temperature, which in the present experiment was below the 0°C to 27°C range validated in their paper. Neglecting the Parrish and Prausnitz model, it is evident that the model predictions for samples CMsI, CMsII, and HMsI trend lower than dissociation pressures determined acoustically. This discrepancy is likely caused by the use of a strong brine in the experiment, as this level of salinity is not taken into account in any of the models. The models may have failed to accurately predict dissociation pressures because they did not fully account for the activity of the fluid molecules surrounding the sample. Although the presence of simple salts does not directly affect the hydrate's enthalpy of formation, dissolved ions in the fluid decrease the entropy

sample	structure	f_{meas} [kHz]	ρ [kg/m^3]	K [GPa]
CMsI	sI	0.1 to 3.5	1029	2.8
CMsII	sII	0.1 to 3.5	2050	0.4
HMsI	sI	0.1 to 3.5	1497	0.3
GMsII	sII	0.1 to 3.5	1326	1.7
Lee et al.	sI	500 to 800	920	6.4
Helgerud et al.	sI	not given	900	7.9
Waite et al.	sI	1000	900	7.7 ± 0.5
Pandit and King	sI	820	750 to 850	5.7 ± 0.1

Table 3: Properties of methane hydrate samples of the present experiment compared to values determined by Lee et al. (Ref [18]), Helgerud et al. (Ref. [19]), Waite et al. (Ref. [20]), and Pandit and King (Ref. [21]). Frequency range used in measurement is indicated by f_{meas}.

of the water molecules, thus decreasing dissociation temperatures [15]. As temperature was held constant in the present experiment, and hydrate dissociation pressure and temperature have an inverse relationship, the high-salinity brine effectively increased the pressure at which the hydrate samples became unstable. A striking observation, then, is each of the models' seemingly accurate predictions of the dissociation pressure of sample GMsII. The sample was suspended in a brine of 132‰ salinity, yet all three models predict dissociation pressures within 6% of the acoustically-determined value. Here, we are likely seeing not impressive accuracy of the models, but a coincidence of two opposing errors. The first error is caused by the salinity of the host solution, which raises dissociation pressure, and the second error relates to the chemical composition of the gas in the hydrate samples. An overview of the major components of the gas in the samples is given in Table 1. While the gas in samples CMsI and HMsI was almost purely methane, and over 80% of the gas in sample CMsII was methane, sample GMsII contained a gas comprised of less than 30% methane. Lu et al. experimentally found a relationship between the gas composition and the stability of a hydrate, showing that stucture I hydrates containing nearly pure methane were the least stable, while structure II hydrates with significant propane and butane constituents dissociated at much lower pressures [9].

Although several models are available to describe the temperature-pressure relationship of hydrate stability, the models have limited ranges of validity, and often do not account for the structure of the hydrate or its surrounding medium. Moreover, many of the available models have been developed as fits to a relatively small bank of experimental data. Further development of stability models and new laboratory investigations of hydrate behavior are necessary to fully map the phases of hydrates in arbitrary media.

In addition to measurement of hydrate dissociation pressures, bulk moduli of the stable gas hydrate samples were measured using Wood's model of a two-phase mixture (Eq. 6). Measured values are presented alongside values found in the literature in Table 3. Inspection of the data shows values of low-frequency bulk moduli which are far below previously measured values. Three possible explanations are presented to account for this discrepancy. First, during the experiment the video monitor used to measure brine column height became clouded with an oily film which was released from the hydrate samples. This may have resulted in inaccurate measurements of hydrate sample density and volume fraction—two key terms in the expression used to calculate the bulk modulus. For the four samples of the present experiment, an estimate of the length uncertainty is ± 2 mm in liquid level, which would result in 12% to 28% error in bulk modulus measurement.

The oily substance released from the hydrate samples is an indicator of a second potential source of error—impurity. A pure gas hydrate

would contain only H_2O-ice and gas molecules, and should have an appearance similar to ordinary water ice, yet the samples tested in the present work visibly contained a significant mud and clay content. This could explain the high density measurements of the samples. However, the literature shows that values of sediment bulk moduli are typically similar to or greater than the established values we have seen for gas hydrates [22, 23, 24]. Wood's model defines the effective bulk modulus of a medium as a linear combination of the bulk moduli of the constituents of the medium. Therefore, any presence of high-bulk-modulus sediment in a sample should result in a measurement of the effective bulk modulus of the sample which is equal to or greater than the bulk modulus of the hydrate in the sample. Thus, we can assume that the low measured values of bulk moduli were not a result of the presence of sediment in the samples.

The most plausible explanation for the differences we see between bulk moduli measured in the present experiment and values from the literature stems from the very motivation of this work: It is known that gassy sediments and composites can exhibit highly frequency-dependent behavior, such that the acoustic velocity of a gassy sediment at high frequencies may be more than an order of magnitude greater than its acoustic velocity below the resonance frequency of the gas bubbles in the sediment [25, 26]. From the expression for the speed of compressional sound propagation through a solid,

$$c(\omega) = \sqrt{\frac{K(\omega) + \frac{4}{3}G(\omega)}{\rho}}, \qquad (13)$$

where G is the shear modulus of the solid, we see that a frequency-dependent sound speed implies highly frequency-dependent elastic moduli. For example, the tenfold difference between low- and high-frequency sound speeds which has been observed in gassy sediments relates to a hundredfold difference in elastic moduli. Given the vast difference between the frequencies used in the present experiment and the measurement frequencies found in the literature, it is plausible that all of the bulk moduli listed in Table 3—the established high-frequency values, as well as the low-frequency values of the present experiment—are correct. It is likely that the frequency-dependent behavior of the elastic moduli of methane hydrates is the primary cause of the differences between bulk moduli which have been measured at ultrasonic frequencies and the values measured in this work.

Additional Work

Despite the known frequency dependence of the acoustic properties of gassy substances, and despite a discrepancy between the low frequencies used to locate gas hydrates and the high frequencies most often used to characterize them, few experiments have investigated the low-frequency acoustic properties of gas hydrates.

The promising results of this experiment give cause to continue work on low-frequency acoustics of gas hydrates. The authors intend to perform similar measurements on synthetic sI and sII hydrate samples. The purity of synthetic samples will allow for more accurate characterization of the low-frequency properties of the materials and better calibration of the measurement technique. In future experiments, temperature and hydrostatic pressure will be varied independently to more fully map the phase boundaries of gas hydrates using low-frequency acoustic techniques.

REFERENCES

[1] G. Rehder, P.W. Brewer, E.T. Peltzer, and G. Friederich. Enhanced lifetime of methane bubble streams within the deep ocean. *Geophysical Research Letters*, 29(15):21–1, 2002.

[2] K.U. Heeschen, A.M. Tréhu, R.W. Collier, E. Suess, and G. Rehder. Distribution and height of methane bubble plumes on the Cascadia Margin characterized by acoustic imaging. *Geophysical Research Letters*, 30(12):1643, 2003.

[3] E.J. Sauter, S.I. Muyakshin, J.L. Charlou, M. Schlüter, A. Boetius, K. Jerosch, E. Damm, J.P. Foucher, and M. Klages. Methane discharge from a deep-sea submarine mud volcano into the upper water column by gas hydrate-coated methane bubbles. *Earth and Planetary Science Letters*, 243(3-4):354–365, 2006.

[4] H.M. Powell. The structure of molecular

compounds; clathrate compounds. *Journal of the Chemical Society*, 16:61, 1948.

[5] E.D. Sloan and C.A. Koh. *Clathrate Hydrates of Natural Gases*. CRC, 2008.

[6] E.D. Sloan Jr. Physical/chemical properties of gas hydrates and application to world margin stability and climatic change. *Geological Society London Special Publications*, 137(1):31, 1998.

[7] R. Sassen and I.R. MacDonald. Evidence of structure H hydrate, Gulf of Mexico continental slope. *Organic Geochemistry*, 22(6):1029–1032, 1994.

[8] P.S. Wilson, A.H. Reed, W.T. Wood, and R.A. Roy. The low-frequency sound speed of fluid-like gas-bearing sediments. *The Journal of the Acoustical Society of America: Express Letters*, 123:99–104, 2008.

[9] H. Lu, Y. Seo, J. Lee, I. Moudrakovski, J.A. Ripmeester, N.R. Chapman, R.B. Coffin, G. Gardner, and J. Pohlman. Complex gas hydrate from the Cascadia margin. *Nature*, 445(7125):303–306, 2007.

[10] V.A. Del Grosso. Analysis of multimode acoustic propagation in liquid cylinders with realistic boundary conditions—Application to sound speed and absorption measurements. *Acústica*, 24(6):299–311, 1971.

[11] P.S. Wilson, A.H. Reed, J.C. Wilbur, and R.A. Roy. Evidence of dispersion in an artificial water-saturated sand sediment. *The Journal of the Acoustical Society of America*, 121:824, 2007.

[12] A.B. Wood. *A Textbook of Sound: Being an Account of the Physics of Vibrations with Special Reference to Recent Theoretical and Technical Developments*. G. Bell and Sons, Ltd., 1930.

[13] W.R. Parrish and J.M. Prausnitz. Dissociation pressures of gas hydrates formed by gas mixtures. *Industrial & Engineering Chemistry Process Design and Development*, 11(1):26–35, 1972.

[14] J.H. van der Waals and J.C. Platteeuw. Clathrate solutions. *Advances in Chemical Physics*, 2:1–57, 1959.

[15] G.R. Dickens and M.S. Quinby-Hunt. Methane hydrate stability in seawater. *Geophysical Research Letters*, 21(19):2115–2118, 1994.

[16] E.T. Peltzer and P.G. Brewer. Practical physical chemistry and empirical predictions of methane hydrate stability. *Natural Gas Hydrate in Oceanic and Permafrost Environments*, pages 17–28, 2000.

[17] C.A. Greene. Low-Frequency Acoustic Classification of Methane Hydrates. Master's thesis, The University of Texas at Austin, Austin, TX, United States, 2010.

[18] M.W. Lee, D.R. Hutchinson, T.S. Collett, and W.P. Dillon. Seismic velocities for hydrate-bearing sediments using weighted equation. *Journal of Geophysical Research*, 101(B9):20347, 1996.

[19] M.B. Helgerud, J. Dvorkin, A. Nur, A. Sakai, and T. Collett. Elastic-wave velocity in marine sediments with gas hydrates: Effective medium modeling. *Geophysical Research Letters*, 26(13):2021–2024, 1999.

[20] W.F. Waite, M.B. Helgerud, A. Nur, J.C. Pinkston, L.A. Stern, S.H. Kirby, and W.B. Durham. Laboratory measurements of compressional and shear wave speeds through methane hydrate. *Annals of the New York Academy of Sciences*, 912(1):1003–1010, 2000.

[21] B.I. Pandit and M.S. King. Elastic wave propagation in propane gas hydrates. In *Proceedings of the 4th Canadian Permafrost Conference*, pages 335–342, 1982.

[22] D. Gei and J.M. Carcione. Acoustic properties of sediments saturated with gas hydrate, free gas and water. *Geophysical Prospecting*, 51(2):141–158, 2003.

[23] J.A. Priest, A.I. Best, and C.R.I. Clayton. A laboratory investigation into the seismic velocities of methane gas hydrate-bearing sand. *Journal of Geophysical Research*, 110(B4):B04102, 2005.

[24] M.D. Richardson, K.L. Williams, K.B. Briggs, and E.I. Thorsos. Dynamic measurement of sediment grain compressibility at atmospheric pressure: acoustic applications. *IEEE Journal of Oceanic Engineering*, 27(3):593–601, 2002.

[25] S.N. Domenico. Elastic properties of unconsolidated porous sand reservoirs. *Geo-*

physics, 42:1339, 1977.

[26] A.L. Anderson and L.D. Hampton. Acoustics of gas-bearing sediments. II. Measurements and models. *The Journal of the Acoustical Society of America*, 67:1890–1903, 1980.